Available online at www.sciencedirect.com
SCIENCE DIRECT®
Chemical Physics Letters 385 (2004) 486–490
CHEMICAL PHYSICS LETTERS
www.elsevier.com/locate/cplett

The substitution reactions $RH + O_2 \rightarrow RO_2 + H$: transition state theory calculations based on the ab initio and DFT potential energy surface

G.A. Bogdanchikov [a,b], A.V. Baklanov [a,b,*], D.H. Parker [c]

[a] Institute of Chemical Kinetics and Combustion, Institutskaya St. 3, Novosibirsk 630090, Russia
[b] Novosibirsk State University, Novosibirsk 630090, Russia
[c] University of Nijmegen, Toernooiveeld 1, Nijmegen 6525 ED, The Netherlands

Received 19 November 2003; in final form 9 January 2004

Abstract

The new class of substitution reactions with oxygen molecule as an agent has been studied by combination of quantum chemistry calculation and transition state theory (TST). The 'inversion substitution' processes $RH + O_2 \rightarrow RO_2 + H$ ($R = CH_3$ and SiH_3) have been investigated. The energy for the stationary points (reagents, products and transition states) on the reaction coordinate has been calculated by G2M(CC,MP2) method and rate constants have been calculated within TST approach. The results show that in methane case the reaction considered ($CH_4 + O_2 \rightarrow CH_3O_2 + H$) does not compete with generally accepted mechanism ($CH_4 + O_2 \rightarrow CH_3 + HO_2$), but it does at elevated temperature in silane case.

1. Introduction

The chemical reactions of oxygen with organic and inorganic molecules are of crucial importance for the chemistry of atmosphere, combustion chemistry, biochemistry as well as for chemical plant processes. The open shell oxygen molecule initiates formation of active radicals giving rise to the chain oxidation processes. When the substrate molecule has C–H or generally X–H bond, this initiation step is considered to be the abstraction reaction. For example, in the processes of combustion or more generally oxidation of saturated hydrocarbons, RH, the first oxygen-assisted step, is accepted to proceed via the abstraction of hydrogen atoms by oxygen molecule [1–4]

$$RH + O_2 \rightarrow R + HO_2 \quad (1)$$

In the current Letter, we study the other mechanism of radicals generation in $RH + O_2$ reaction which involves homolytic substitution process

$$RH + O_2 \rightarrow RO_2 + H \quad (2)$$

The homolytic substitution reactions

$$RX + Y \rightarrow RY + X \quad (3)$$

are well known for the case of Y being the atom. Most of the previous studies for these reactions have been done for reaction $H' + CH_4 \rightarrow CH_3H' + H$ [5, and references therein]. In the paper, Niblaues et al. [5] have used UHF and CI methods for calculation of CH_5 hypersurface and found that this reaction proceeds via Walden-type inversion (inversion substitution) when H′ atom attacks towards the carbon atom from behind the CH bond to be ruptured and collinear with it. So, calculated energy barrier was found to be in a reasonable agreement with experimental data. The existing experimental data for the wide variety of atomic substitution reactions (3) are reviewed in the recent paper by Denisov and Azatyan [6]. The reasonable agreement of experimental data with those calculated within parabolic model with 'inversion substitution' mechanism involved has been achieved by these authors. The open shell nature of molecular oxygen has allowed us to expect that O_2 molecule can be involved in the homo-

* Corresponding author. Fax: +73832342350.
E-mail address: baklanov@ns.kinetics.nsc.ru (A.V. Baklanov).

0009-2614/$ - see front matter © 2004 Published by Elsevier B.V.
doi:10.1016/j.cplett.2004.01.015

lytic substitution reactions (3) similar to the ones for atoms.

In this Letter, substitution reaction (2) with two substrates differing by the central sp^3-hybridized atom ($R = CH_3$ and SiH_3) is studied. For the potential energy surface (PES) calculation, we have applied G2M modification of the GAUSSIAN 2 model. Transition state theory (TST) has been used for calculations of the rate constants for these reactions. The competition of the substitution reaction (2) with the abstraction reaction (1) is also considered for the molecules involved.

2. Calculations

For reactions $RH + O_2 \rightarrow RO_2 + H$ ($R = CH_3$, SiH_3), we have used the G2M(CC,MP2) modification by Mebel et al. [7] of the well-known GAUSSIAN 2 (G2) theoretical model by Pople and coworkers [8]. The calculations within the G2M(CC,MP2) model involve several steps: the calculations of the geometry, vibrational wavenumbers and zero-point vibrational energy (ZPE) within B3LYP approach; electron correlation evaluation using the coupled-cluster method CCSD(T); correction for nonadditivity of diffuse and higher polarization basis set functions within Møller–Plesset second-order method (MP2) and higher-level correction for valence electrons (HLC).

The final energy values have been calculated with the use of equations similar to those of [7]:

$$E[\mathrm{G2M(CC,MP2)}] = E[\mathrm{CCSD(T)/6\text{-}311G(d,p)}] + \Delta E(+3\mathrm{df},2\mathrm{p}) + \Delta E(\mathrm{HLC}) + \mathrm{ZPE[B3LYP/6\text{-}311G(d,p)}],$$

$$\Delta E(+3\mathrm{df},2\mathrm{p}) = E[\mathrm{MP2/6\text{-}311{+}G(3df,2p)}] - E[\mathrm{MP2/6\text{-}311G(d,p)}],$$

$$\Delta E(\mathrm{HLC}) = -0.00019 \cdot n_\alpha - 0.00530 \cdot n_\beta.$$

The symbols n_α and n_β designate the number of α and β valence electrons in the system under consideration.

It is worth mentioning that the model G2M(CC, MP2) provides agreement with experimental thermochemical parameters at the same level of accuracy as G2 model does and gives better results for high spin radicals and provides better results also for geometry and vibrational wavenumbers [7].

To elucidate the competition of the substitution reactions (2) with the abstraction reactions (1), the last ones have been studied for all the substrates by the same G2M(CC,MP2) method.

All the calculations have been carried out with the use of GAUSSIAN package 98 [9] on the SGI Origin 3800 1024 node system of SARA Computing and Networking Services in Amsterdam.

3. Results and discussion

3.1. The justification of G2M(CC,MP2) model application

To illustrate the accuracy provided by G2M(CC, MP2) model application, we have compared the results with the thermochemical parameters calculated earlier within different models of G family as well as those obtained experimentally. The species O_2, CH_4, CH_3, SiH_4 and SiH_3 have been considered. The total atomization energy ($\sum D_0$) and bond strength D_0 have been used for comparison. In Table 1, the results of our G2M(CC,MP2) calculations are given together with those obtained by Pople and coworkers [8] with the use of G2, G2(MP2) [10] and G1 [11,12] schemes.

As it is seen in Table 1, the thermochemical parameters calculated within all the models considered agree with experimental data within 1 kcal/mol (with taking into account the experimental uncertainty) for all species with only exception for O_2. For the last one, the same level of accuracy is provided by only G2M(CC,MP2) model which we used then in our calculations.

Table 1
Total atomization energy $\sum D_0$ and bond strength D_0 in kcal/mol calculated within different models

		G2M (CC,MP2)[a]	G2 [8]	G2(MP2) [10]	G1 [8]	Experiment[b]
Total atomization energy $\sum D_0$	O_2	117.8	115.6	115.9	115.4	118.0 ± 0.0
	CH_4	392.3	393.2	392.7	391.0	392.4 ± 0.2
	CH_3	288.1	289.1	288.7	287.4	289.1 ± 0.2
	SiH_4	304.8	304.8	304.7	304.4	302.5 ± 2.3
	SiH_3	213.5	213.5	213.4	213.1	211.2 ± 4.3
Bond strength D_0	$CH_4 \rightarrow CH_3 + H$	104.3	104.0	104.0	103.7	103.3 ± 0.2
	$SiH_4 \rightarrow SiH_3 + H$	91.3	91.3	91.3	91.4	91.3 ± 2.8

[a] The results of our calculations.
[b] The results obtained with the use of enthalpies of formation at 0 K from [13].

Table 2
Geometry (bond distances in Å, angles in deg), rotational constants and vibrational wavenumbers in cm^{-1} calculated at the B3LYP/6-311G(d,p) level within G2M(CC,MP2) model

Molecule	Geometry	Rotational constants	Vibrational wavenumbers (scaling factor 0.9614)
O_2	$r_{OO} = 1.206$	1.450 (2)	1579
	$\{r_{OO} = 1.2075\}$[a]	{1.438 (2)}[a]	{1580}[a]
CH_4	$r_{CH} = 1.091$, $\angle HCH = 109.5$	5.272 (3)	1290 (3), 1501 (2)
	$\{r_{CH} = 1.094$, $\angle HCH = 109.5\}$[a]	{5.241 (3)}[a]	2910, 3012 (3)
			{1306 (3), 1534 (2) 2917, 3019 (3)}[a]
O_2CH_3H	$r_{OOz} = 1.273$, $r_{ZOz} = 1.677$, $r_{ZX} = 1.785$	1.572	104, 337, 433, 480, 609
$[O_2ZH_3X]$[b]	$r_{ZHz} = 1.083$, $r_{ZH} = 1.082$, $\angle ZO_ZO = 112.5$	0.282	1038, 1064, 1159, 1238
	$\angle O_ZZX = 179.0$, $\angle O_ZZH_Z = 98.6$	0.252	1357, 1360, 2968, 3127
	$\angle O_ZZH = 100.2$, $\angle XZH_Z = 80.4$, $\angle XZH = 80.3$		3129
O_2CH_3	$r_{OOz} = 1.317$, $r_{ZOz} = 1.449$, $r_{ZHz} = 1.089$	1.758	138, 475, 879, 1086, 1110
$[O_2ZH_3]$[b]	$r_{ZH} = 1.090$, $\angle ZO_ZO = 111.2$, $\angle O_ZZH_Z = 105.5$	0.376	1170, 1389, 1413, 1426
	$O_ZZH = 109.0$	0.330	2930, 3017, 3032
SiH_4	$r_{SiH} = 1.484$, $\angle HSiH = 109.5$	2.849 (3)	887 (3), 943 (2), 2149
	$\{r_{SiH} = 1.480$, $\angle HSiH = 109.5\}$[a]	{2.865 (3)}[a]	2157 (3)
			{914 (3), 975 (2), 2187 2191 (3)}[a]
O_2SiH_3H	$r_{OOz} = 1.319$, $r_{ZOz} = 1.796$, $r_{ZX} = 1.969$	1.182	139, 221, 225, 264, 552
$[O_2ZH_3X]$[b]	$r_{ZHz} = 1.479$, $r_{ZH} = 1.478$, $\angle ZO_ZO = 112.7$	0.182	698, 743, 832, 870, 879
	$\angle O_ZZX = 176.7$, $\angle O_ZZH_Z = 99.0$	0.168	1105, 2149, 2177, 2179
	$\angle O_ZZH = 103.8$, $\angle XZH_Z = 77.8$, $\angle XZH = 77.8$		
O_2SiH_3	$r_{OOz} = 1.343$, $r_{ZOz} = 1.737$, $r_{ZHz} = 1.479$	1.179	160, 236, 636, 658, 733
$[O_2ZH_3]$[b]	$r_{ZH} = 1.477$, $\angle ZO_ZO = 108.9$, $\angle O_ZZH_Z = 103.5$	0.214	910, 916, 927, 1107, 2175
	$\angle O_ZZH = 108.6$	0.193	2191, 2195

[a] Experiment [13].
[b] Designation of atoms corresponds to Fig. 1.

3.2. The results of geometry calculations for the stationary points on reaction coordinate for the process $RH + O_2 \rightarrow RO_2 + H$ ($R = CH_3$, SiH_3)

In Table 2, the calculated structure parameters for the stationary points on reaction coordinate are presented for the species of interest together with the available experimental data.

The results of calculations show that C_S symmetry is conserved along the reaction coordinate for the processes under consideration.

The transition state (TS) O2ZH3X (Z = C, Si, X = H) geometry is shown schematically in Fig. 1. As compared with the reagents $O_2 + ZH_3X$, the TS geometry is characterized by lengthening of Z–X bond and partial inversion of Z atom hybridization (see Table 2). In Table 2, the vibrational wavenumbers are also given. The presented calculated values are obtained with the use of scaling factor 0.9614 recommended [13] for the vibrational wavenumbers received within B3LYP approach.

As it is seen from the upper table, the calculated structural parameters are in reasonable agreement with the experimental ones.

3.3. The reaction energy profile calculations

The reagents, products and transition states energy for the reactions

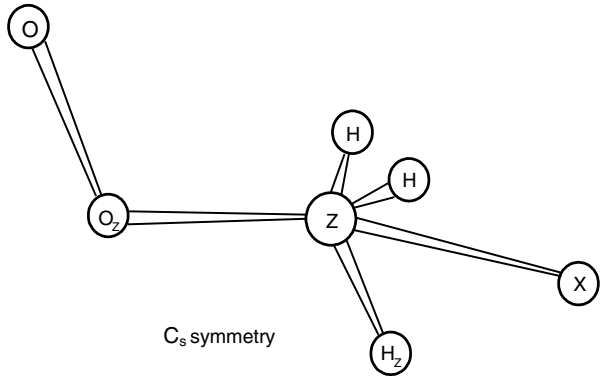

Fig. 1. Scheme of the structure of the transition state for the 'inversion substitution' reaction $O_2 + ZH_3X \rightarrow O_2ZH_3 + X$.

$$O_2 + ZH_4 \rightarrow O_2ZH_3 + H \ (Z = C, Si) \quad (4)$$

have been calculated within the G2M(CC,MP2) model. The results obtained are shown in Fig. 2. For comparison, the calculated parameters for reactions are given

$$ZH_4 \rightarrow ZH_3 + H \ (Z = C, Si) \quad (5)$$

as well. The recombination process reverse to reaction (5) has no activation barrier. The hydrogen loss energy for oxygen assisted reaction (4) is lower by 17 and 43.9 kcal/mol for C and Si as compared with reaction (5).

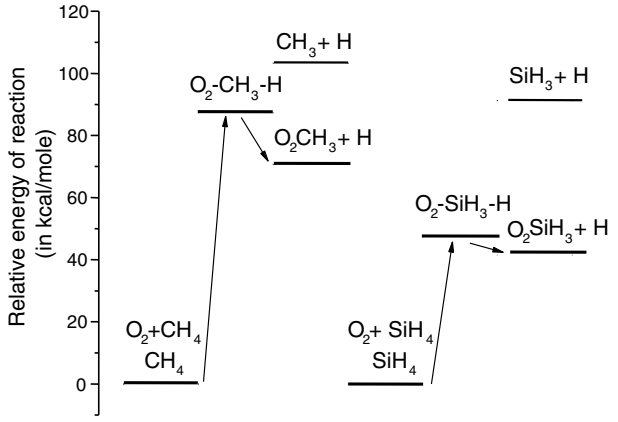

Fig. 2. The relative energy diagram for the 'inversion substitution' $O_2 + ZH_4 \rightarrow O_2ZH_3 + H$ and dissociation $ZH_4 \rightarrow ZH_3 + H$ reactions.

3.4. Rate constant calculations

The rate constant calculations for the reactions under study have been carried out within formalism of TST. All the necessary structural and energy parameters for reagents and transition states have been taken from Table 2. The rate constants have been calculated within the temperature interval from 273 to 2000 K. The temperature dependence of the rate constants $k(T)$ has been fitted by two widely used expressions:

$$k = A \cdot \left(\frac{T}{1000}\right)^n \cdot \exp(-E_0/RT), \tag{6}$$

$$k_A = A_{\text{eff}} \cdot \exp(-E_a/RT). \tag{7}$$

Here, E_0 is the energy difference of TS and reagents.

The results for substitution reactions as well as for the reverse processes are given in Table 3. Both types of the processes were considered to proceed on the triplet potential energy surface. To elucidate the competition of the substitution reaction with the abstraction one in Table 4, the results of energy barrier (E_0) calculation for all these reactions are presented. As it is seen from this Table, E_0 values coincide with the endoergicity values for all the abstraction reactions. The existing experimental data for methane case where the abstraction reaction enthalpy of 54.7 kcal/mol is close to the Arrhenius activation energy of 56.9 kcal/mol [2,3] agrees well with this result. The comparison of E_0 values for substitution and abstraction reactions shows that abstraction reaction dominates in methane case. In silane case the substitution should be already taken into account at high temperature. On the basis of these results, we can conclude that the 'substitution inversion' reaction (2) with oxygen molecule as an agent can be important in initiating the combustion or more generally oxidation of substances.

Table 4
Calculated reaction barrier E_0 and enthalpy at 0 K ΔH_0^0

Reaction	E_0 (kcal/mol)	ΔH_0^0 (kcal/mol)
$CH_4 + O_2 \rightarrow O_2CH_3 + H$[a]	87.3	70.7
$CH_4 + O_2 \rightarrow CH_3 + HO_2$[a]	54.9	54.9 {54.7}[b]
$SiH_4 + O_2 \rightarrow O_2SiH_3 + H$[a]	47.4	41.5
$SiH_4 + O_2 \rightarrow SiH_3 + HO_2$[a]	41.9	41.9 {42.7}[b]

[a] Calculated within G2M(CC,MP2) approach.
[b] The results obtained with the use of enthalpies of formation from [13].

4. Conclusions

The new class of the substitution reactions $RH + O_2 \rightarrow RO_2 + H$ ($R = CH_3$, SiH_3) has been studied with the combination of the ab initio and DFT calculation of the potential energy surface (PES) and transition state theory (TST) for the calculations of the rate constant. These reactions proceed via Walden-type inversion of the pyramidal fragment CH_3 or SiH_3 (so-called 'inversion substitution' mechanism). The substantial drop in the activation energy barrier has been revealed for these reactions relative to the unimolecular dissociation $RH \rightarrow R + H$. The rate constant as a function of temperature was calculated for upper substitution reactions. The results show that in methane case, the reaction considered ($CH_4 + O_2 \rightarrow CH_3O_2 + H$) does not compete with generally accepted mechanism ($CH_4 + O_2 \rightarrow CH_3 + HO_2$). In silane case, the abstraction still dominates but the substitution should notably contribute at high temperature. We can conclude that the considered 'inversion substitution' reactions with molecular oxygen as an agent can be important in the chemistry of atmosphere and combustion.

Table 3
The kinetic parameters resulted from the fitting of calculated $k(T)$ by Eqs. (6) and (7)

Reaction	$A \times 10^{12}$	n	E_0	$A_{\text{eff}} \times 10^{12}$	E_a
$O_2 + CH_4 \rightarrow O_2CH_3 + H$	43.0 ± 2.3	1.96 ± 0.07	87.3	165 ± 33	89.6 ± 0.2
$O_2CH_3 + H \rightarrow O_2 + CH_4$	40.2 ± 0.8	1.02 ± 0.03	16.6	81.6 ± 7.6	17.8 ± 0.1
$O_2 + SiH_4 \rightarrow O_2SiH_3 + H$	49.9 ± 1.8	2.38 ± 0.05	47.4	266 ± 53	50.1 ± 0.2
$O_2SiH_3 + H \rightarrow O_2 + SiH_4$	52.3 ± 0.8	1.14 ± 0.02	5.9	117 ± 10	7.3 ± 0.1

A and A_{eff} are given in cm^3/s. E_0 and E_a are given in kcal/mol.

Acknowledgements

The authors gratefully acknowledge the financial support of this work by the Dutch National Science foundation NWO (Grant No. 047.009.011) as well as support by Russian Foundation of Basic Research (Grant No. 02-03-32001) and Russian Ministry of Education (Grant No. E02-3.2-51). The computing time on the SGI Origin 3800 system of SARA Computing and Networking Services in Amsterdam was provided by the Dutch National Computer Facility NCF.

References

[1] J. Warnatz, in: W.C. Gardiner (Ed.), Combustion Chemistry, Springer, New York, 1984.
[2] W. Tsang, R.F. Hampson, J. Phys. Chem. Ref. Data 15 (1986) 1087.
[3] D.L. Baulch, C.J. Cobos, R.A. Cox, P. Frank, G. Hayman, T. Just, J.A. Kerr, T. Murrels, M.J. Pilling, J. Troe, R.W. Walker, J. Warnatz, J. Phys. Chem. Ref. Data 23 (1994) 847.
[4] E.T. Denisov, T.G. Denisova, Rus. Chem. Rev. 71 (2002) 417.
[5] K. Niblaeus, B.O. Roos, P.E.M. Siegbahn, Chem. Phys. 26 (1977) 59.
[6] E.T. Denisov, V.V. Azatyan, Kinet. Catal. 44 (2003) 1.
[7] A.M. Mebel, K. Morokuma, C. Lin, J. Chem. Phys. 103 (1995) 7414.
[8] L.A. Curtiss, K. Raghavachari, G.W. Trucks, J.A. Pople, J. Chem. Phys. 94 (1991) 7221.
[9] M.J. Frish et al., GAUSSIAN 98, Revision A.9, Gaussian Inc., Pittsbutgh, PA, 1998.
[10] L.A. Curtiss, K. Raghavachari, J.A. Pople, J. Chem. Phys. 98 (1993) 1293.
[11] J.A. Pople, M. Head-Gordon, D.J. Fox, K. Raghavachari, L.A. Curtiss, J. Chem. Phys. 90 (1989) 5622.
[12] L.A. Curtiss, C. Jones, G.W. Trucks, K. Raghavachari, J.A. Pople, J. Chem. Phys. 93 (1990) 2537.
[13] National Institute of Standards and Technology (NIST). Computational Chemistry Comparison and Benchmark Data Base (CCCBDB). Available from: http://srdata.nist.gov/cccbdb/.